Forecasting rodent population dynamics and community transitions with dynamic nonlinear models

Nicholas J. Clark, S. K. Morgan Ernest, Henry Senyondo, Juniper L. Simonis, Ethan P. White, Glenda M. Yenni, K. A. N. K. Karunarathna

Supplementary Materials

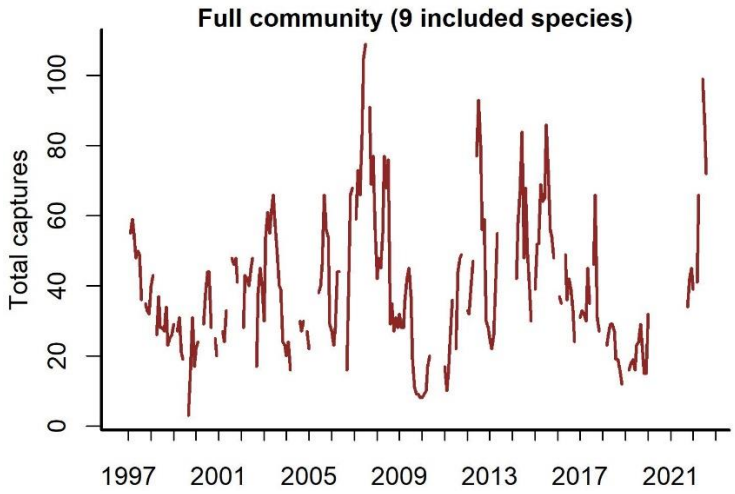

Figure S1: Total rodent captures from the Portal Project for the period December 1996 to August 2022. Counts represent total captures for nine species across 10 control plots, sampled monthly. Blanks represent missing values.

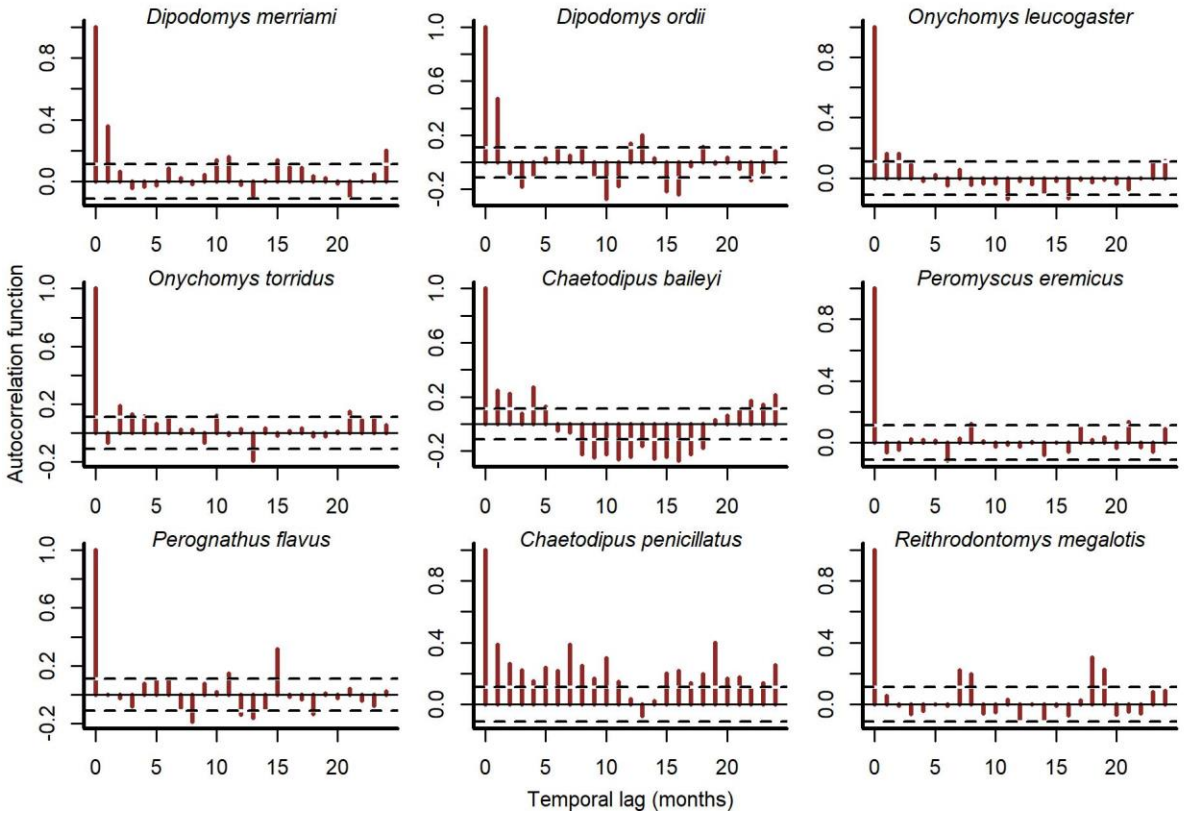

Figure S2: Autocorrelation functions of rodent capture time series in the Portal Project. Dashed lines show values beyond which the autocorrelations are considered significantly different from zero.

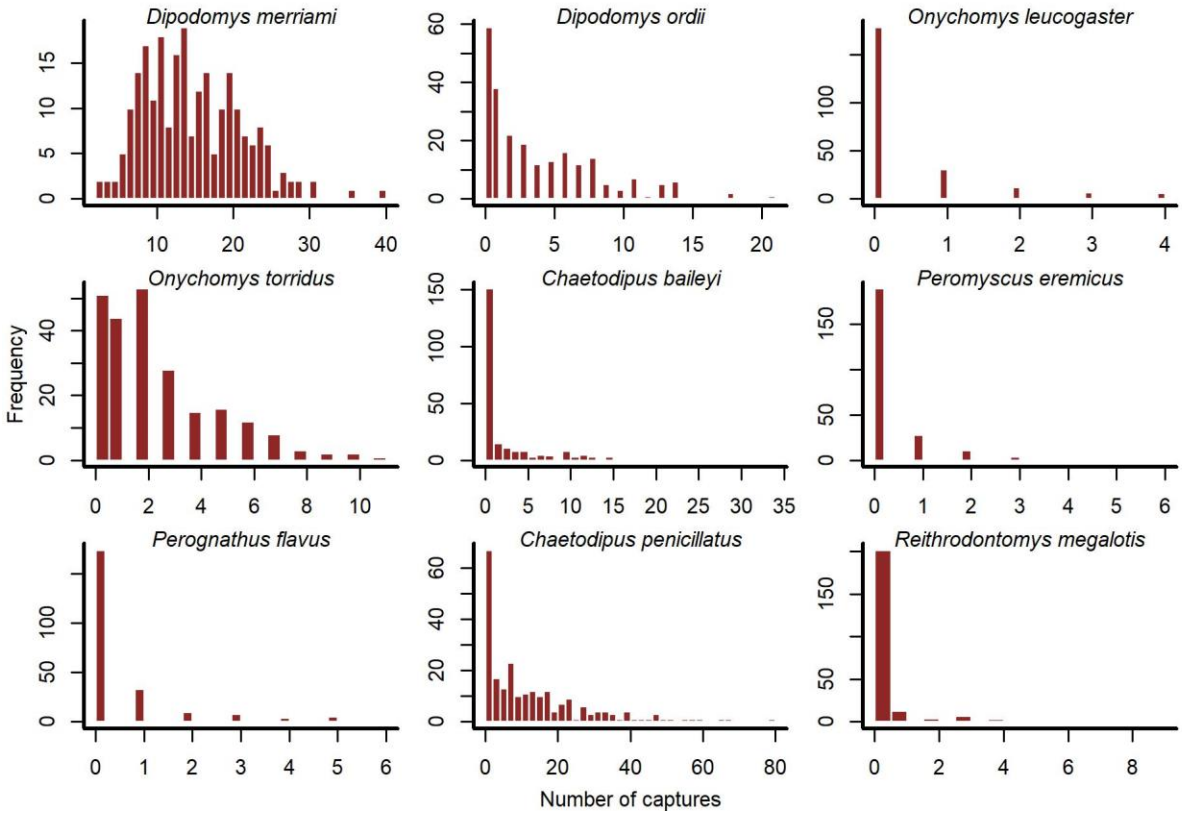

Figure S3: Histograms of rodent capture time series in the Portal Project. Counts represent total captures across 10 control plots, sampled monthly.

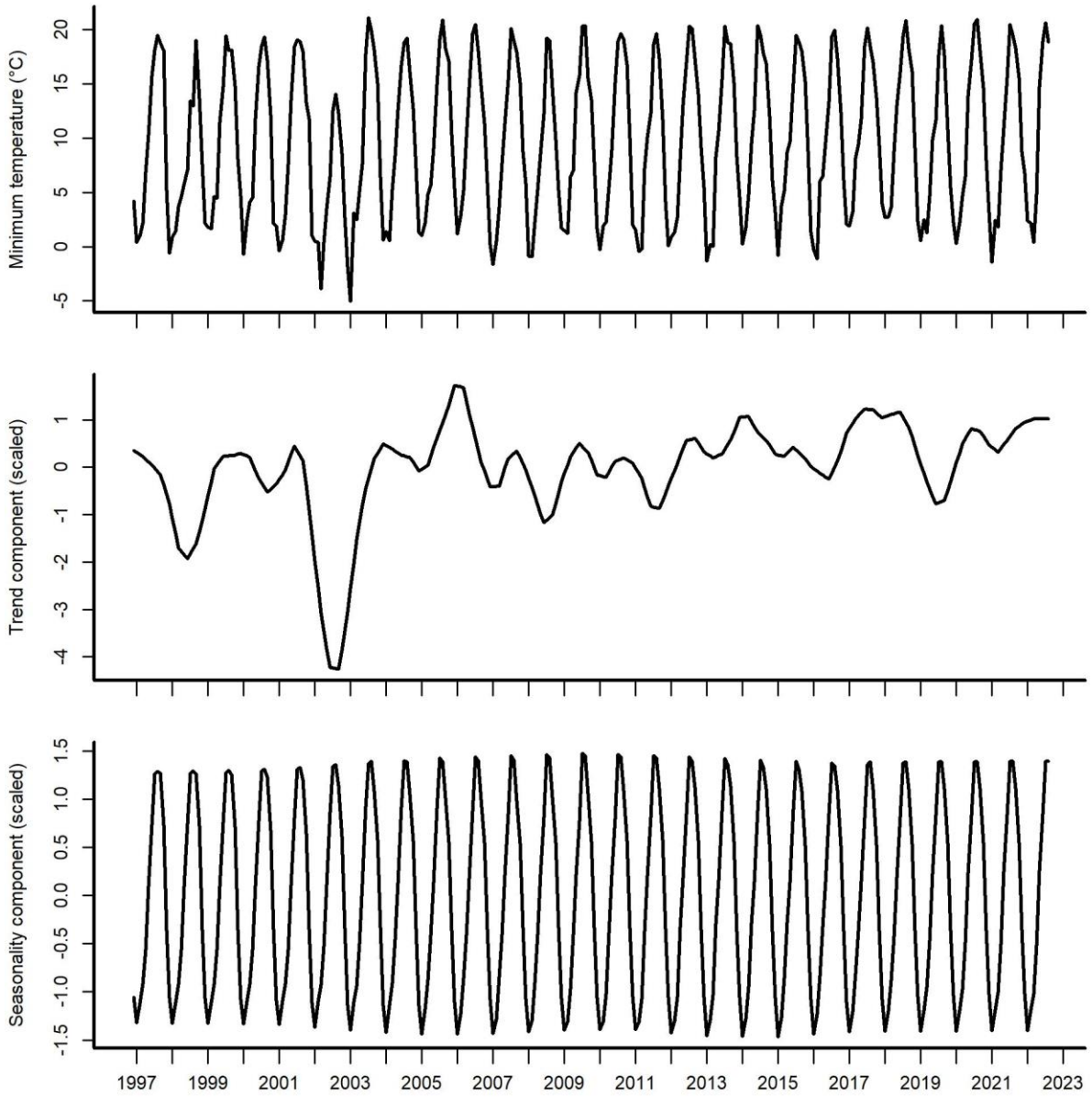

Figure S4: Seasonal and Trend decomposition using Loess smoothing (STL) applied to observed minimum temperature time series for the period December 1996 – August 2022. The top panel shows the raw time series. The middle plot shows the estimated long-term trend (calculated using a Loess regression to the de-seasoned time series). The bottom plot shows the time-varying estimate of seasonality (calculated using a Loess regression that smooths across years). STL components were estimated using the *msts()* function in the *forecast* R package (Hyndman and Khandakar 2008).

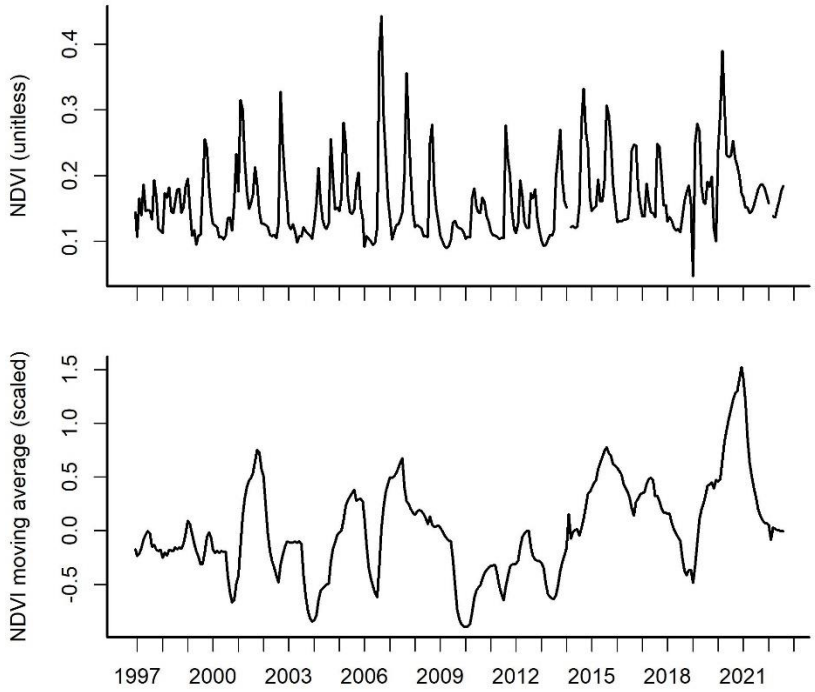

Figure S5: Top panel: observed Normalized Difference Vegetation Index (NDVI) time series for the period December 1996 – August 2022, with obvious seasonal fluctuations. Bottom panel: a 12-month moving average that represents smooth, gradual changes in NDVI at the study site.

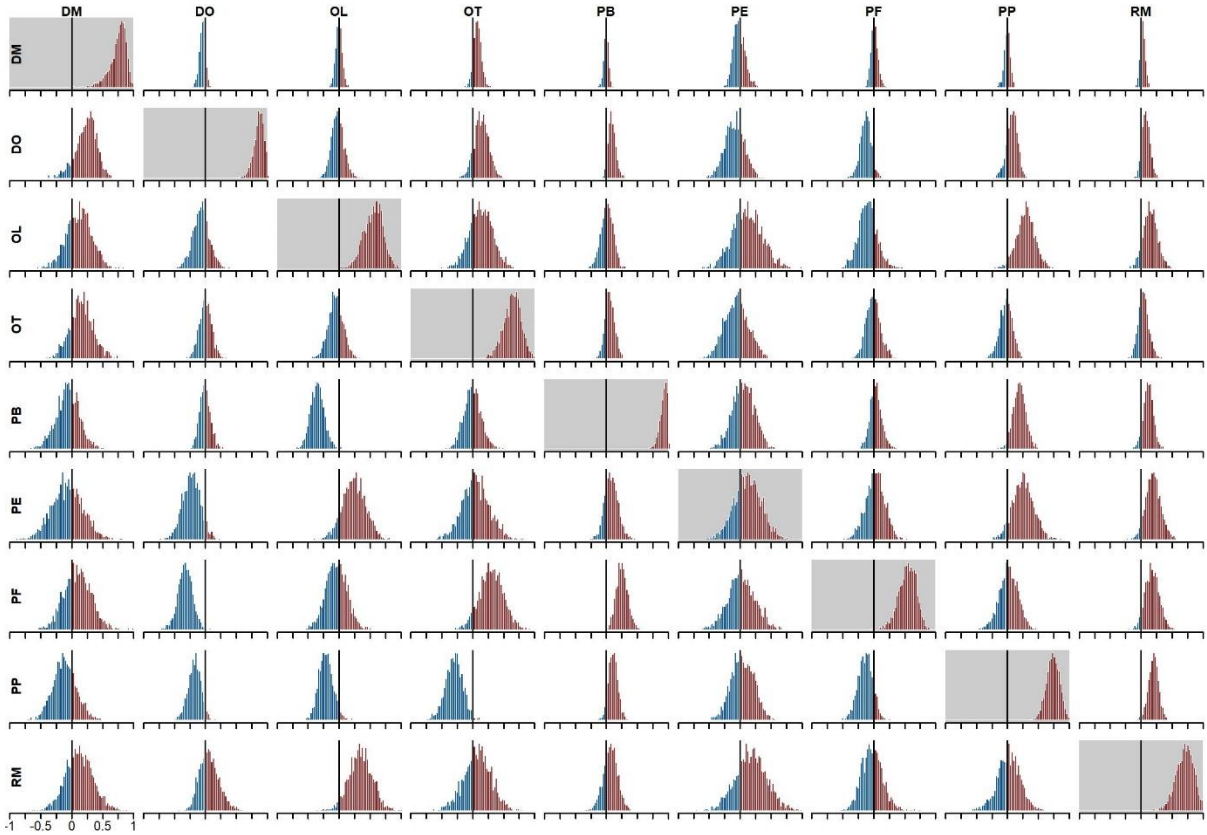

Figure S6: Posterior distributions of vector autoregressive coefficients (matrix $\boldsymbol{A}$). Off-diagonals represent cross-dependencies. For example, the entry in $\boldsymbol{A}[\mathbf{1},\mathbf{2}]$ captures the effect of **DO**'s trend at time $t-1$ on the current trend for **DM** (at time t). Diagonals (with grey shading) represent autoregressive coefficients (the effect of a species' trend at time $t-1$on its own trend at time t). Colours indicate the proportion of probability mass at or below zero (in blue) vs above zero (in red). **DO**, *Dipodomys merriami*; **DO**, *Dipodomys ordii*; **OL**, *Onychomys leucogaster*; **OT**, *Onychomys torridus*; **PB**, *Chaetodipus baileyi*; **PE**, *Peromyscus eremicus*; **PF**, *Perognathus flavus*; **PP**, *Chaetodipus penicillatus*; **RM**, *Reithrodontomys megalotis*.

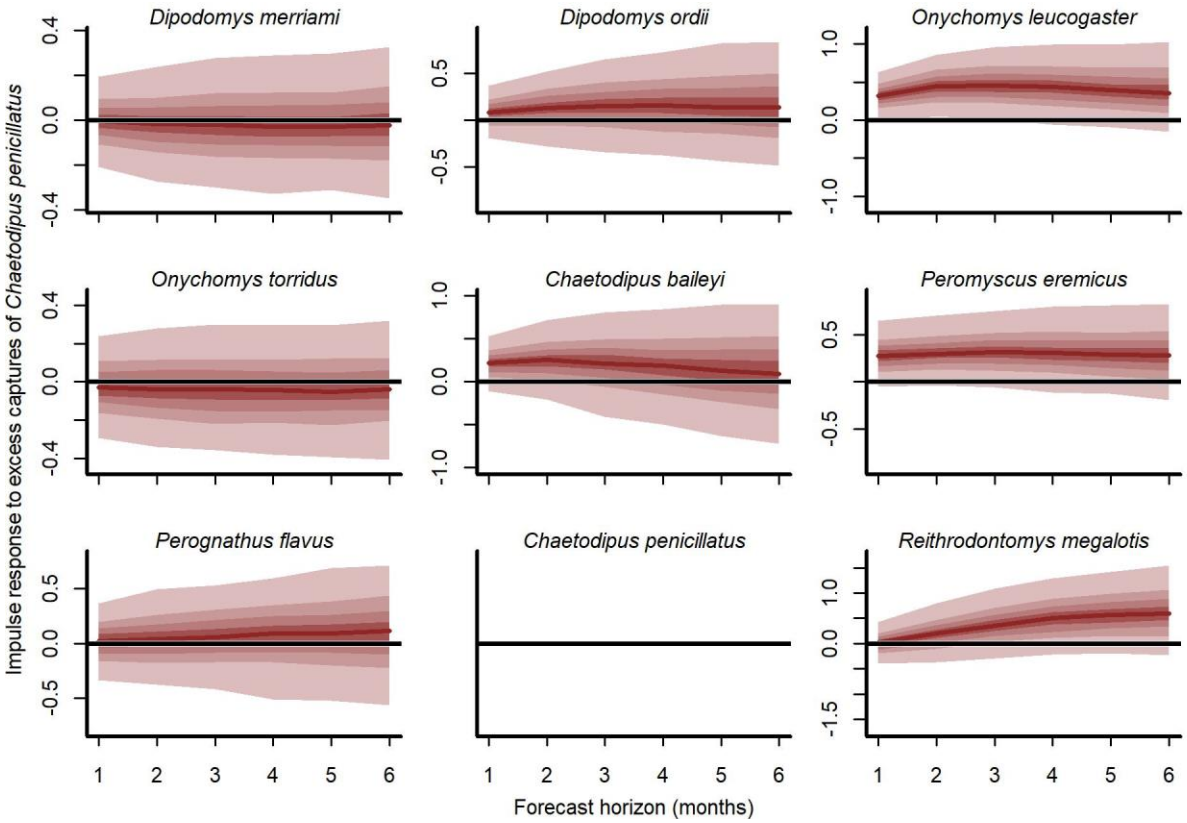

Figure S7: Expected responses to a pulse in captures of the desert pocket mouse (*Chaetodipus penicillatus*). Ribbon plots show how mean captures (μ, on the log scale) are expected to change over the next six months if three additional *C. penicillatus* individuals are captured. Ribbon shading shows posterior empirical quantiles (90th, 60th, 40th and 20th). Dark red lines show posterior medians.

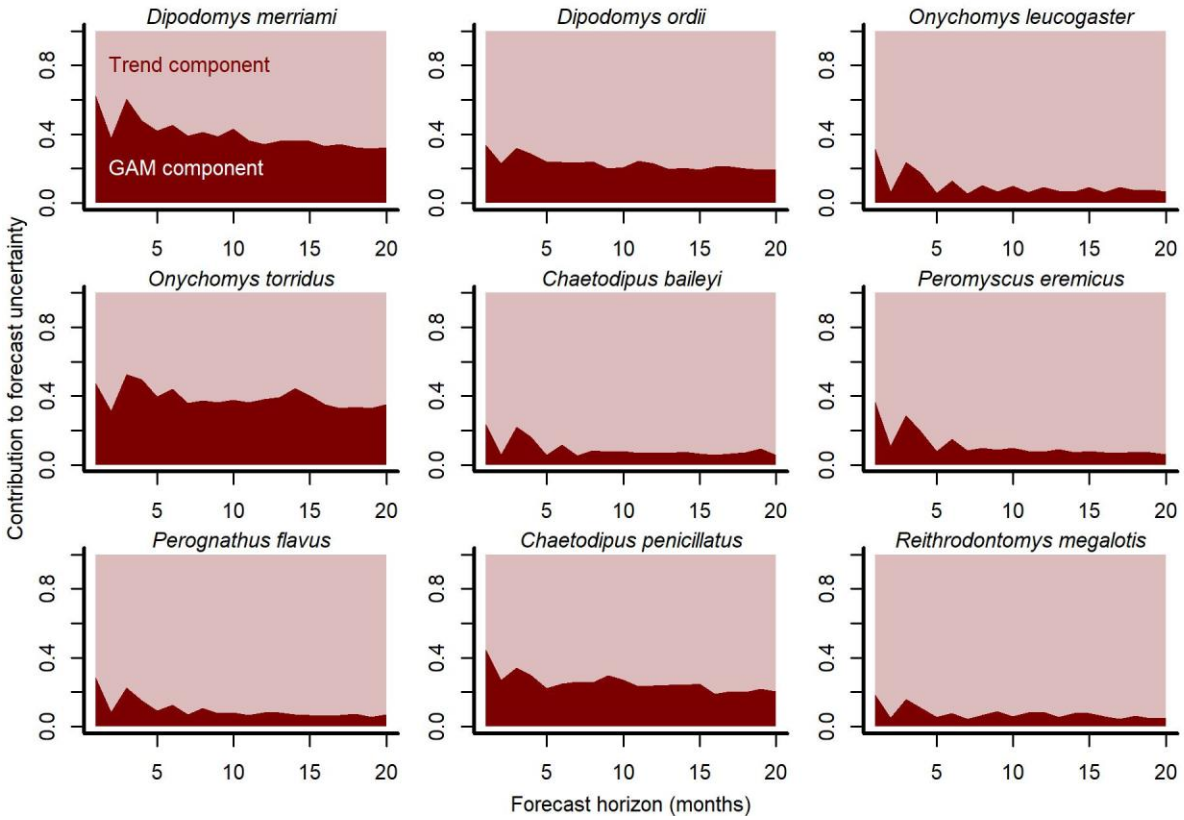

Figure S8: Relative contributions of uncertainty in the latent trend and GAM components of the linear predictor to forecast uncertainty over increasing forecast horizons.

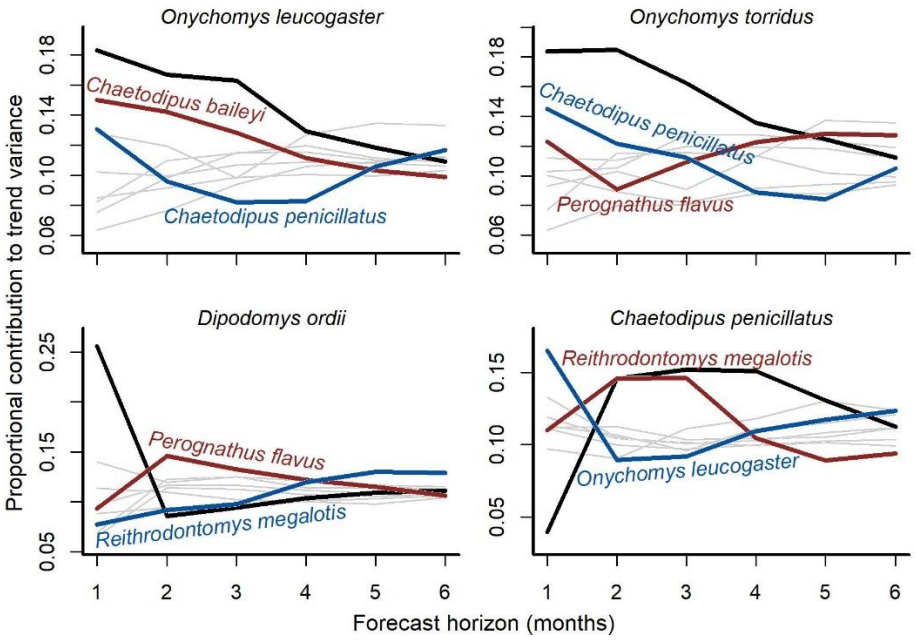

Figure S9: Latent trend variance decompositions for a few species. Each line shows the relative contribution of a sudden pulse in captures at time zero to the focal species' trend variance over a six-month forecast horizon. Black lines show relative contributions of pulses for the focal species on their own trend variance. Other lines show relative contributions of pulses for the remaining species in the community. Interesting relationships are highlighted in colour. Pulses were simulated as an excess of three captures at time zero.

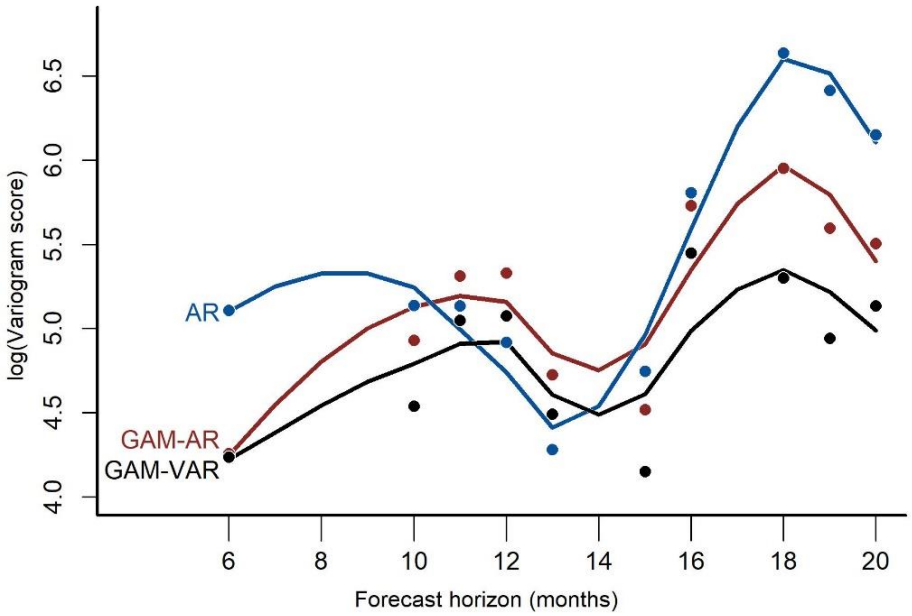

Figure S10: Out of sample forecast performances of competing models. Y-axis shows the log of the variogram score, a proper score that penalizes multivariate forecasts if they do not capture correlations in observed data. Forecasts were evaluated on 24 out of sample time points (years 2021 and 2022). Points show scores. Lines show Loess smoothed trendlines. Missing values were used for timepoints when sampling did not occur. A lower score indicates a better forecast.

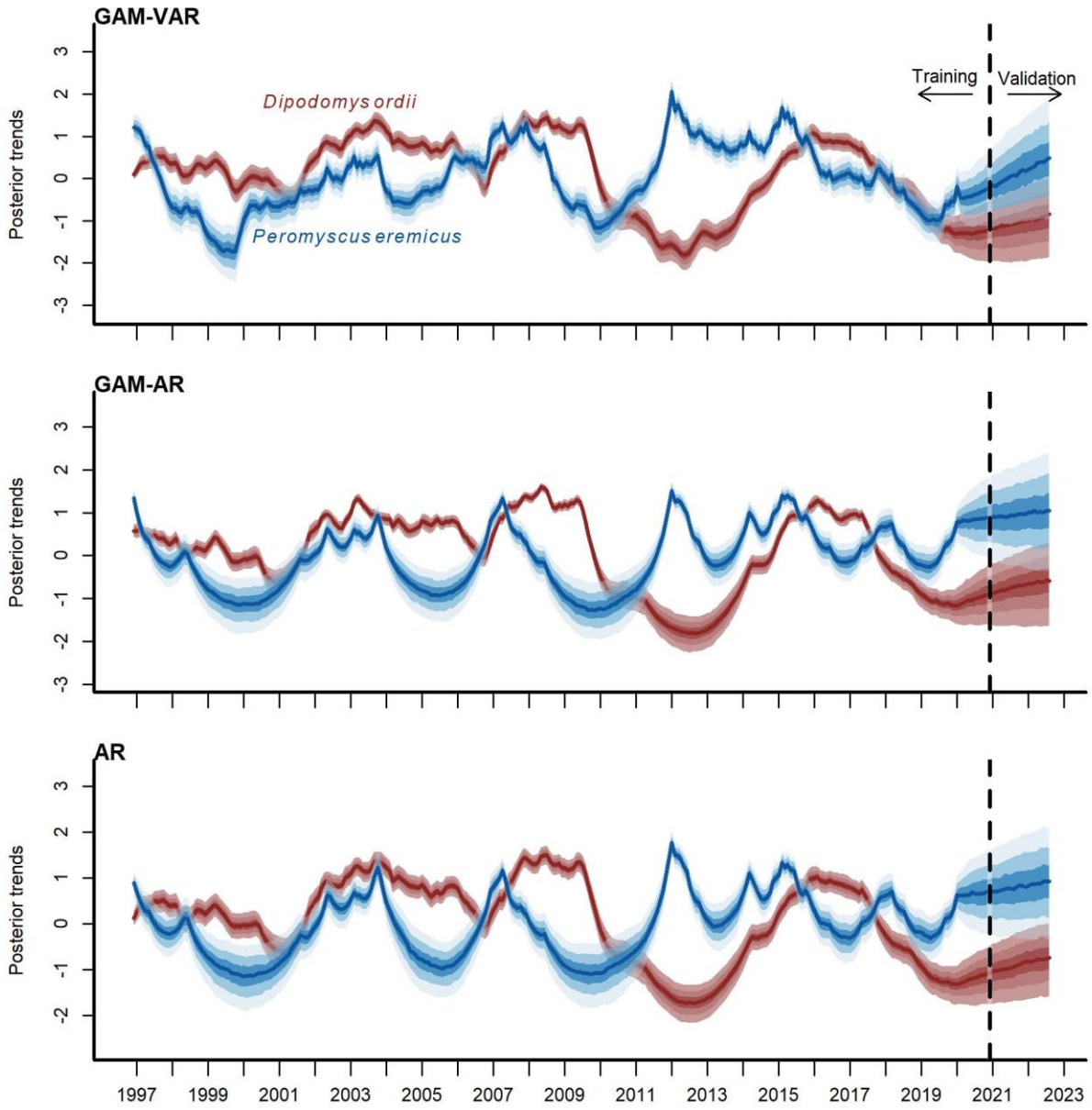

Figure S11: Posterior trend estimates from three competing models for Ord's kangaroo rat (*Dipodomys ordii*; in red) and cactus mouse (*Peromyscus eremicus*; in blue). Trends were scaled to unit variance for comparisons. Ribbon shading shows posterior empirical quantiles (90th, 60th, 40th and 20th). Dark lines show posterior medians.

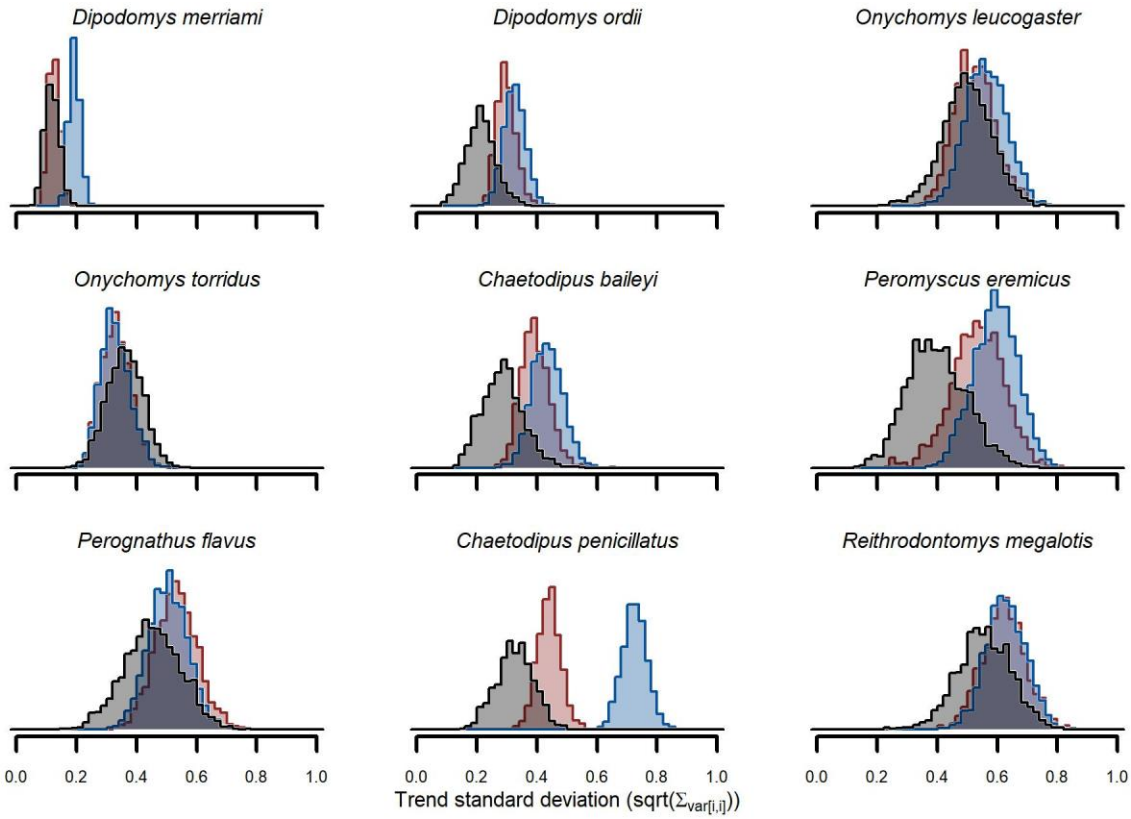

Figure S12: Posterior estimates of trend standard deviations from the three competing models. Estimates are the square root of diagonal parameters from the trend covariance matrix ($\boldsymbol{\Sigma_{VAR}}$) for the ***GAM-VAR*** (black), ***GAM-AR*** (red) and ***AR*** (blue).

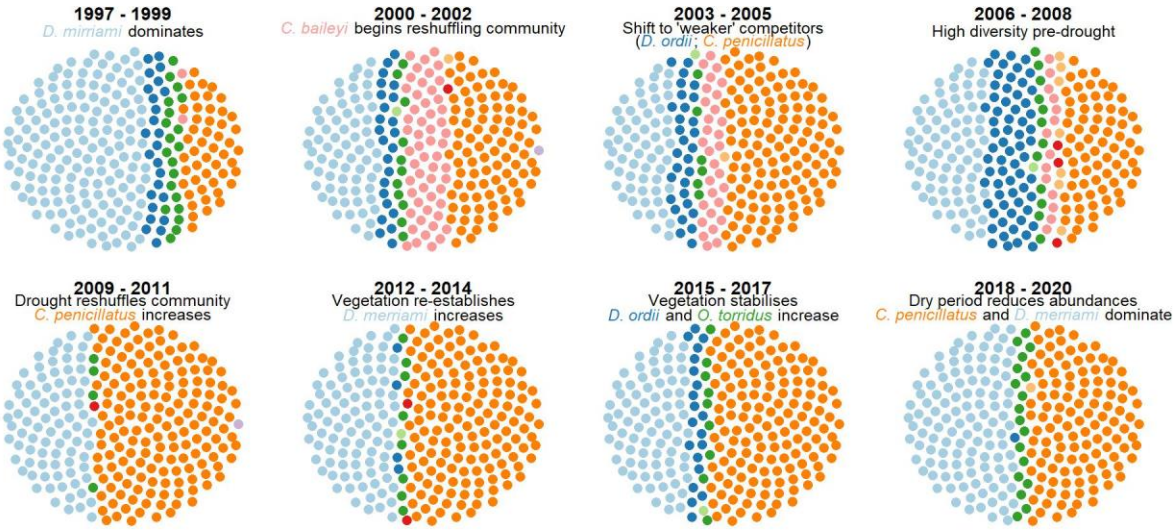

Figure S13: Simulated rodent communities. Using the ***GAM-VAR*** model's posterior predictive distribution, we simulated communities of 200 individuals at different timepoints to investigate how well the model captured known community transitions. Colours represent different species.

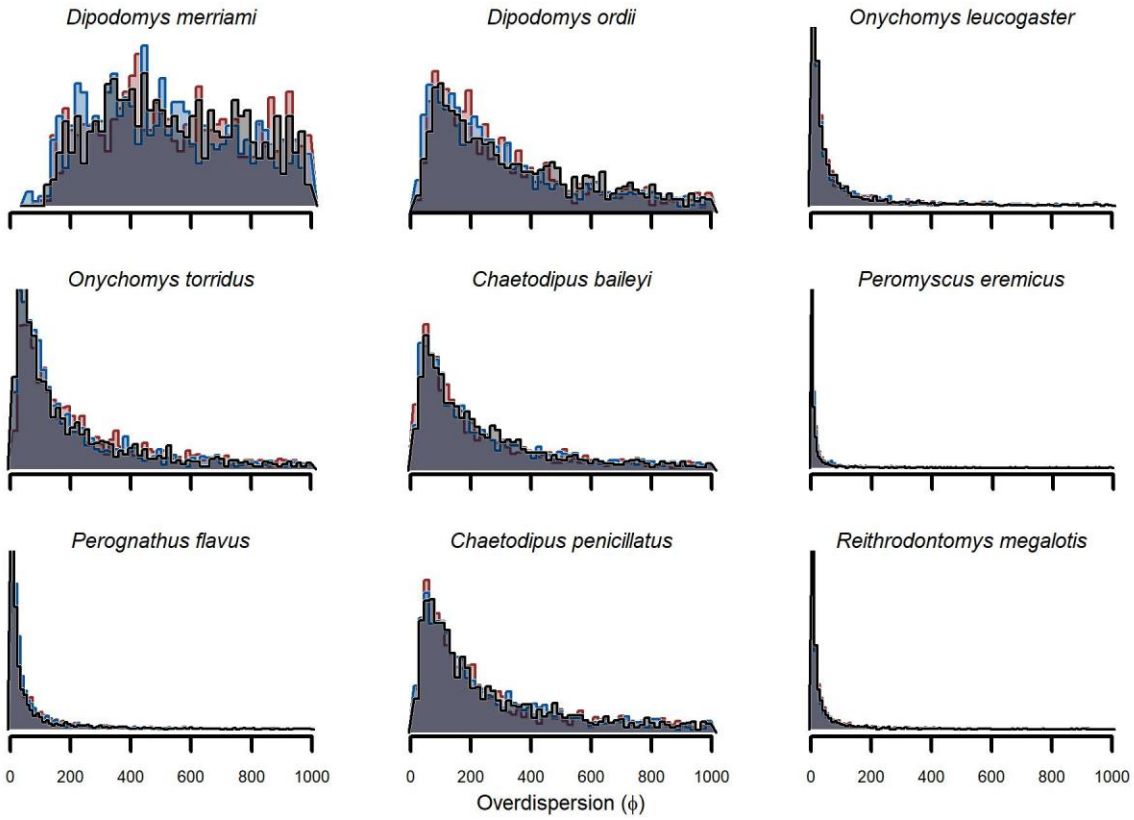

Figure S14: Posterior estimates of Negative Binomial overdispersion parameters from the ***GAM-VAR*** (black), ***GAM-AR*** (red) and ***AR*** (blue). Smaller values of Φ indicate a larger amount of overdispersion.

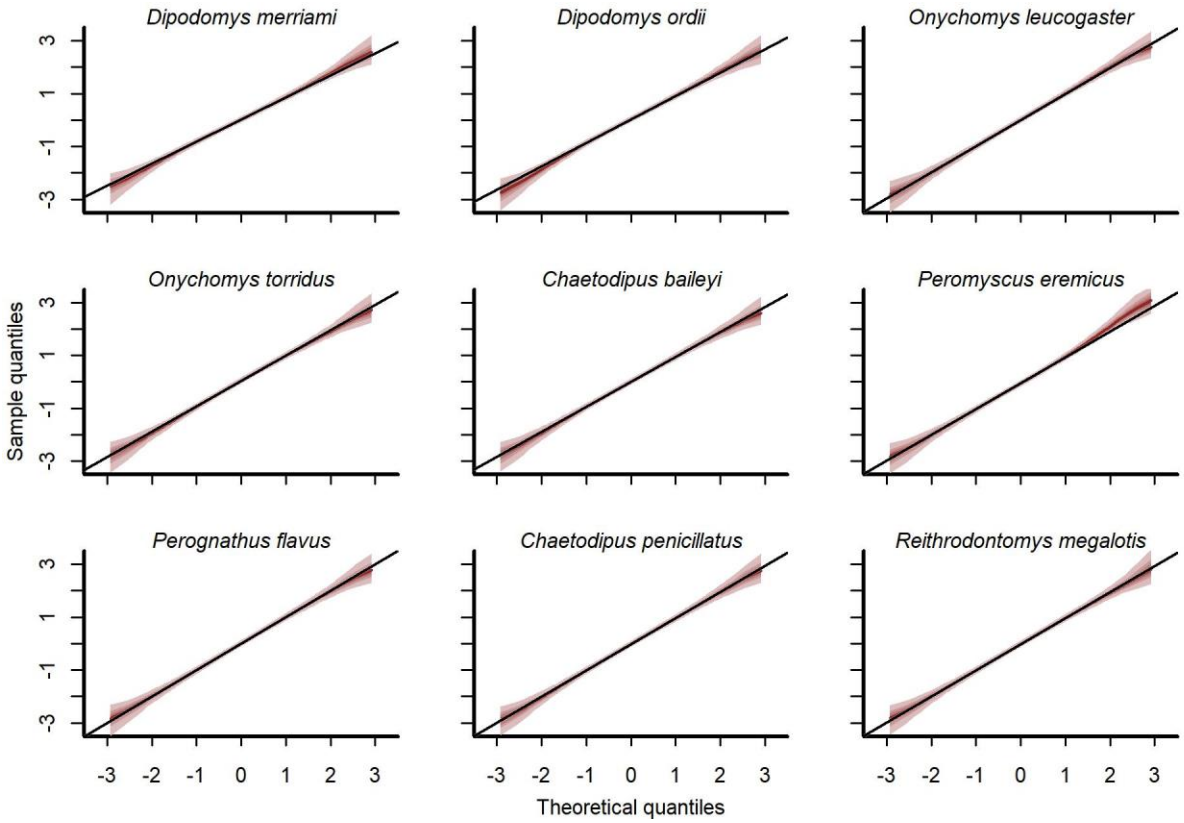

Figure S15: Normal quantile-quantile plots of randomized quantile residuals. Ribbon shading shows posterior empirical quantiles (90th, 60th, 40th and 20th). Dark lines show posterior medians.

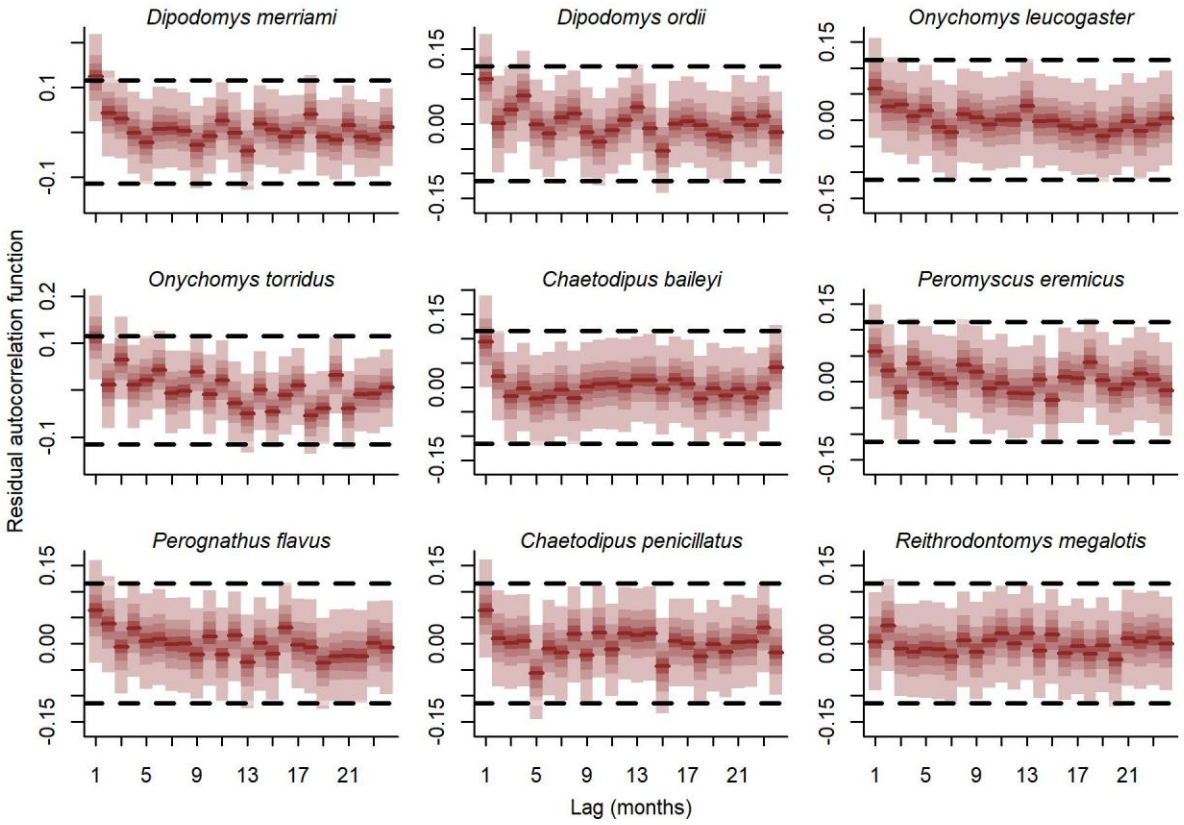

Figure S16: Autocorrelation functions of randomized quantile residuals. Ribbon shading shows posterior empirical quantiles (90th, 60th, 40th and 20th). Dark red lines show posterior medians. Dashed lines show values beyond which the autocorrelations would be considered significantly different from zero in a Frequentist paradigm.

References

Hyndman, R. J., and Y. Khandakar. 2008. Automatic time series forecasting: the forecast package for R. Journal of Statistical Software **27**:1-22.